

# Transient Negative Species in Supercritical Carbon Dioxide: Electronic Spectra and Reactions of CO<sub>2</sub> Anion Clusters<sup>†</sup>

Kenji Takahashi,<sup>\*,‡,§</sup> Sadashi Sawamura,<sup>‡</sup> Nada M. Dimitrijevic,<sup>§</sup> David M. Bartels,<sup>§</sup> and Charles D. Jonah<sup>\*,§</sup>

Argonne National Laboratory, 9700 South Cass Avenue, Argonne, Illinois 60439, and Division of Quantum Energy Engineering, Hokkaido University, Sapporo 060-8628, Japan

Received: June 19, 2001; In Final Form: October 2, 2001

Transient absorption spectra following ionization of supercritical CO<sub>2</sub> have been investigated using the pulse radiolysis technique. Absorption spectra measured from 400 to 800 nm suggest that at least two transient species absorb. We have previously reported that one species is (CO<sub>2</sub>)<sub>2</sub><sup>+</sup>. In the near UV region, we observed a transient species of which the lifetime and reactivity are different from the dimer cation. We assign this species to a dimer anion, (CO<sub>2</sub>)<sub>2</sub><sup>-</sup>, or an anion–molecule complex, (CO<sub>2</sub><sup>-</sup>)(CO<sub>2</sub>)<sub>x</sub>. Comparison with the photobleaching of CO<sub>2</sub> anion clusters in solid rare gas matrixes and their reactivity with H<sub>2</sub> and O<sub>2</sub> confirm the assignment. Theoretical calculations, in which solvation is taken into account, are consistent with these assignments. It is well-established that the adiabatic electron affinity of CO<sub>2</sub> is negative, but the adiabatic electron affinity of CO<sub>2</sub> dimer has been calculated to be 0.89 eV for *D*<sub>2d</sub> symmetry (CO<sub>2</sub>)<sub>2</sub><sup>-</sup> in the gas phase. The calculations predict that CO<sub>2</sub><sup>-</sup> in a model continuum solvent is stable to autodetachment.

## 1. Introduction

There have been extensive efforts to understand the characteristics of supercritical fluids as solvents.<sup>1,2</sup> Energy-transfer and electron-transfer reactions have also been used as a probe to elucidate the solvent characteristics.<sup>3,4</sup> It has been a challenge to utilize CO<sub>2</sub> in reaction schemes because it is difficult to activate CO<sub>2</sub>.<sup>5</sup> One potential route to activate CO<sub>2</sub> involves reduction of CO<sub>2</sub>.<sup>6,7</sup> This could be achieved by an electron transfer to CO<sub>2</sub> to yield the corresponding anion radical. For this reason, we wanted to explore the existence of the anion and its reactivity.

There have been extensive studies of ion–molecule reactions in gas-phase CO<sub>2</sub>. It is well-established that the primary positive ion in the radiolysis of CO<sub>2</sub> gas is CO<sub>2</sub><sup>+</sup> and that CO<sub>2</sub><sup>+</sup> forms clusters rapidly with CO<sub>2</sub>.<sup>8–10</sup> The atomic oxygen radical anion, O<sup>-</sup>, which is produced by dissociative electron attachment to CO<sub>2</sub>, is known to be the primary negative ion in the high-energy radiolysis.<sup>11–17</sup> To dissociate CO<sub>2</sub> to CO + O<sup>-</sup>, about 4.0 eV of energy is required (calculated from the bonding energy(O–CO) = 5.453 eV, and the electron affinity(O) = 1.461 eV).<sup>18</sup> O<sup>-</sup> will react rapidly with CO<sub>2</sub> to form CO<sub>3</sub><sup>-</sup>. The reactions that electrons with less energy than 4 eV undergo are not yet known. While several studies of negative species in the gas phase exist, there are few reports of the observation of CO<sub>2</sub> anions from the ionization of CO<sub>2</sub> in the gas phase. Even in a liquid and high-density CO<sub>2</sub>, some thought that CO<sub>2</sub><sup>-</sup> was unstable and thus not observable.<sup>19,20</sup> In a mobility experiment by Jacobsen and Freeman, electron attachment to a molecular cluster of CO<sub>2</sub> was assumed.<sup>21</sup> When the density of CO<sub>2</sub> is

greater than 14 × 10<sup>25</sup> molecules/m<sup>3</sup> in the coexistence vapor, the negative and positive charges have the same mobility, so it is expected that the electrons are permanently attached to CO<sub>2</sub>. CO<sub>2</sub><sup>-</sup> has also been observed in a low-pressure glow discharge.<sup>22</sup> Recently, it has been reported that CO<sub>2</sub><sup>-</sup> can be formed by double electron transfer to CO<sub>2</sub><sup>+</sup> in the gas phase.<sup>23</sup> However, to the best of our knowledge, until the recent photolytic measurements by Shkrob and Sauer, there is no other clear evidence that CO<sub>2</sub> anion is formed in condensed or gas-phase CO<sub>2</sub>.<sup>24</sup>

The most widely accepted value for the adiabatic electron affinity of CO<sub>2</sub> in the gas phase is -0.6 ± 0.2 eV.<sup>25</sup> The ab initio calculations also predict a negative electron affinity.<sup>26–29</sup> The absence of CO<sub>2</sub><sup>-</sup> in a low-pressure environment arises from the poor Franck–Condon overlap between the ground states of the neutral CO<sub>2</sub> and its anion. Ground-state CO<sub>2</sub><sup>-</sup> is bent with an O=C=O angle of about 135°, whereas the neutral ground-state CO<sub>2</sub> is linear. Linear CO<sub>2</sub><sup>-</sup>, formed by vertical electron attachment, will be vibrationally excited by 2–3 eV. This species will either autodetach or dissociate in a few femtoseconds. Collisional stabilization of this ion cannot occur in low-pressure conditions.

There have been many studies on carbon dioxide cluster anion formation in molecular beams or van der Waals clusters.<sup>30–36</sup> For example, Klots and Compton<sup>31</sup> demonstrated anion cluster formation in a CO<sub>2</sub> molecular jet, where the dimer anion is formed, presumably by evaporative electron attachment. The ion-signal intensity as a function of incident electron energy has shown a maximum around 3 eV. It is believed that the molecular cluster binds an excess electron differently than the monomer.<sup>37</sup> Although there are still open questions in the formation mechanism of CO<sub>2</sub> anion clusters,<sup>18,38–40</sup> it is generally concluded that a single CO<sub>2</sub> molecule cannot bind an excess electron, whereas a weakly bound CO<sub>2</sub> cluster is able to bind an electron. Several calculations for CO<sub>2</sub>-dimer anion have been made, and three stable isomers with *D*<sub>2d</sub>, *D*<sub>2h</sub>, and *C*<sub>s</sub> structure are predicted.<sup>41–43</sup>

\* To whom correspondence should be addressed. E-mail for K.T.: kenji@pleiades.qe.eng.hokudai.ac.jp. Fax for K.T.: +81-11-706-6675. E-mail for C.D.J.: CDJonah@anl.gov. Fax for C.D.J.: 630-252-4993.

<sup>†</sup> Work was performed under the auspices of the Office of Basic Energy Sciences, Division of Chemical Science, US-DOE under contract number W-31-109-ENG-38.

<sup>§</sup>Argonne National Laboratory.

<sup>‡</sup>Hokkaido University.

According to these experimental facts and theoretical predictions, stable  $\text{CO}_2$  anion or anion clusters could be formed in condensed or supercritical  $\text{CO}_2$ . We have recently studied the reduction of *p*-benzoquinone in supercritical  $\text{CO}_2$  using pulse radiolysis.<sup>44</sup> That work clearly demonstrated that an electron donor has been produced by ionization of supercritical  $\text{CO}_2$ . We tentatively assigned the electron donor to the  $\text{CO}_2$  cluster anion; however, we did not observe any spectra that could be attributed to the anion. This is partly because in the solution a strong absorption by *p*-benzoquinone and its anion overlaps the region where the absorption of the  $\text{CO}_2$  anion cluster might be expected. In addition, the absorption of the anion might be quite small.

In recent experiments using rare gas matrixes, stable  $\text{CO}_2$  monomer anion and its dimer have been observed.<sup>43,45,46</sup> In these studies, the infrared absorption assigned to  $(\text{CO}_2)_2^-$  was decreased by irradiation with visible light. This suggests that an absorption band of  $(\text{CO}_2)_2^-$  in rare gas solid is located in the visible region. These results led us to reexamine spectra produced in supercritical  $\text{CO}_2$ .

In this paper, we will discuss absorption spectra of transient species that we assign to the  $\text{CO}_2$  anion clusters, which were produced by electron beam irradiation in supercritical  $\text{CO}_2$ . We also examined the reactions of the anion cluster with  $\text{H}_2$  and  $\text{O}_2$ . To determine whether the  $\text{CO}_2$  anion will autoionize, ab initio calculations were performed. We believe that these are the first measurements of absorption spectra of  $\text{CO}_2$  anion clusters in supercritical  $\text{CO}_2$ .

Very shortly after our absorption measurements were performed, Shkrob and Sauer<sup>24</sup> studied the mobility of an anion in supercritical  $\text{CO}_2$ . Electrons were created in a supercritical solution by photoionizing benzene or anthracene. To get the aromatics into the supercritical solution conveniently in the appropriate quantities, the aromatics were dissolved in a small amount of hexane and injected into the system. The concentrations of the aromatic and the carrier hexane were sufficiently small that no effect would be expected on the reaction kinetics. They reported evidence that the resulting electron attaches to  $\text{CO}_2$  to form the solvent anion. The photodetachment spectrum observed is reported as similar to photoelectron spectra of the  $(\text{CO}_2)_n^-$  cluster ( $n = 6-9$ ) and consistent with our results for absorption spectrum of the anion clusters. These results can be a bridge between radiolysis and photolysis and between electrons in neat  $\text{CO}_2$  and  $\text{CO}_2$  solutions. It can also advance our understanding of the formation mechanism of the  $\text{CO}_2$  anion cluster in supercritical  $\text{CO}_2$  and  $\text{CO}_2$  solution.

## 2. Experimental Section

The  $\text{CO}_2$  was supercritical fluid chromatography (SFC) grade from Scott Specialty Gases. Impurities in this gas reported by Scott are  $\text{H}_2\text{O}$  (<3 ppm),  $\text{O}_2$  (<2 ppm),  $\text{CO}$  (<5 ppm),  $\text{H}_2$  (5 ppm),  $\text{CH}_4$  (2 ppm),  $\text{N}_2$  (50 ppm), and Ar (5 ppm). It was used as received. The  $\text{H}_2$  (Aldrich, 99.99+%) and  $\text{O}_2$  (AGA, 99.9%) were also used as received.

Experiments were performed in a stainless steel high-pressure cell. Two suprasil windows (1-cm thick, 3-cm diameter) were mounted to the cell using Teflon O-rings and passed the analyzing light and electron beam. The optical path length is 5 cm, and the effective diameter is 1.2 cm (an  $F/\# = 4$ ). The optical densities shown in the figures were not divided by the optical path length. All experiments were done at a constant temperature of  $40.1 \pm 0.1$  °C (a reduced temperature of 1.03 °C) unless otherwise stated. The temperature was controlled and monitored using a temperature controller (Omega, model CN

1001 RTD). The pressure in the cell was adjusted using an HPLC pump (JASCO, model PU-980) and monitored with a digital pressure meter (Cole-Parmer, model 7350-38). Measurements have been carried out at 104 bar, at which the density is 0.65 g/cm<sup>3</sup>, and at 53 bar, at which the density is 0.13 g/cm<sup>3</sup>. The experimental arrangements for supercritical fluids were similar to those described previously.<sup>44</sup>

Pulse radiolysis experiments were performed using the Argonne 20 MeV linear accelerator with electron pulses of 4 ns. For optical detection, interference filters (bandwidth 40 nm) and a silicon photodiode (EG&G FND100) were used. This detection method was chosen over our monochromator/photomultiplier tube system because a better signal-to-noise (S/N) ratio can be obtained. Because the accumulation of radiolytic products prevents extensive signal averaging, a good S/N ratio is quite important. Most of the signals presented here were the average of two single-shot signals. The electron beam and the analyzing light were collinear. This arrangement was chosen to increase the optical path length. However, the electron pulse irradiation to the 10-mm-thick optical windows mounted on the high-pressure cell caused a small absorption. This absorption intensity was about 0.003 at 400 nm, and the half-lifetime was about 200 ns. The window absorption intensities depend on absorbed dose, which is sensitive to the linac beam conditions. Hence, we measured absorption of the optical window by electron beam irradiation before starting the experiments every time, and the absorption signal was corrected by subtracting the signal from the window absorption.

Radiolytic products, mainly, carbon monoxide, ozone, and oxygen, accumulate after the irradiation of several pulses and influence the measurements. To prevent this, the sample was freshly prepared after each irradiation. In some experiments, the measurements were performed under flowing conditions, in which the pressure was controlled by a backpressure regulator (TESCOM 26-1700). However, it was difficult to control the temperature at 40.1 °C and a pressure of 104 bar. Hence, this method was applied only for a measurement at lower temperature and pressure.

## 3. Results and Discussion

In this section, we will first describe the spectra that one observes in pure  $\text{CO}_2$ . We then discuss measurements using  $\text{H}_2$ , which reacts with positive ions, to determine the spectrum that might be associated with an anion. We compare the observed spectrum with results from photobleaching experiments of matrix-isolated anions. Experiments in the presence of oxygen give further information on the species that are observed. Ab initio calculations were used to estimate the energetics of the different species; these results were used to confirm the plausibility of the suggested reactions.

**3.1. Transient Spectra in Pure  $\text{CO}_2$ .** We have already reported that an absorption spectrum can be observed in pure  $\text{CO}_2$  within about 200 ns after the electron pulse.<sup>47</sup> The transient absorption spectra are shown in Figure 1. The absorption spectral shape is broad and the maximum is located around 700 nm. We previously attributed the observed absorption spectrum to  $(\text{CO}_2)_2^+$  by comparing with the photodestruction cross section<sup>48</sup> of  $(\text{CO}_2)_2^+$  and by considering the reactivity of this species with several cation scavengers. Although the absorption spectrum corresponds relatively well to the photodestruction cross section, there is a discrepancy, especially in the blue region. Hence, we thought it possible that another species also was absorbing. Confirming this hypothesis is the shoulder or growth in absorption from 450 to 400 nm that can be seen in Figure 1.

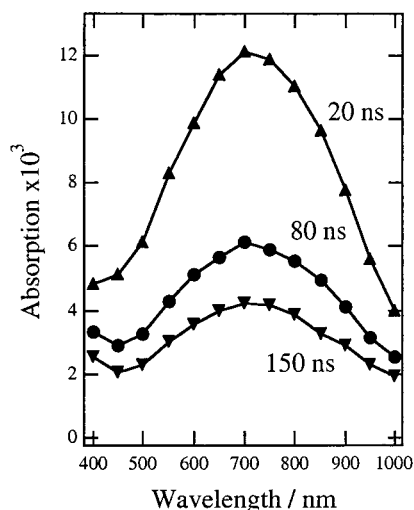


**Figure 1.** Transient absorption spectra observed at 20, 80, and 150 ns after the electron pulse in pure CO<sub>2</sub> at a temperature of 40.1 °C and pressure of 104 bar (density = 0.6 g/cm<sup>3</sup>).

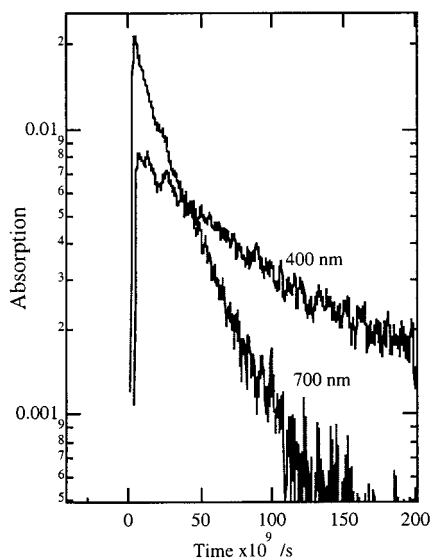


**Figure 2.** Comparison of decay kinetics at 700 nm with those at 400 nm. The temperature is 35 °C, and the pressure is 53 bar (density of 0.13 g/cm<sup>3</sup>).

The 400-nm absorption decays with different kinetics than does the 700-nm absorption.

Figure 2 shows a very clear difference in the kinetics at lower temperature (35 °C). Note that the measurements in this figure were done at a pressure of 53 bar (density = 0.13 g/cm<sup>3</sup>), so the diffusion-controlled reaction of the cation, which is observed at 700 nm, is much faster than the data in Figure 1 (104 bar, 0.65 g/cm<sup>3</sup>). The absorption signal at 700 nm decays faster than the signal at 400 nm. This result clearly demonstrates that the transient species around 700 nm is different from that around 400 nm. We suggest that the spectrum at 400 nm is predominantly due to (CO<sub>2</sub>)<sub>2</sub><sup>+</sup> or (CO<sub>2</sub><sup>-</sup>)(CO<sub>2</sub>)<sub>x</sub>. To establish this assignment, we isolated this spectrum by the addition of compounds that react with the cation. We then compared the resulting spectrum with what is known about the anion spectrum from the literature.

### 3.2. Reactions and Spectra in H<sub>2</sub>/CO<sub>2</sub> Mixture. Reactions.

We have tried to isolate the spectrum of the species that absorbs in the near UV region from the overlapping absorption of the (CO<sub>2</sub>)<sub>2</sub><sup>+</sup>. Using a specific cation scavenger is one way to achieve this. The scavenger and its reacted product should have no

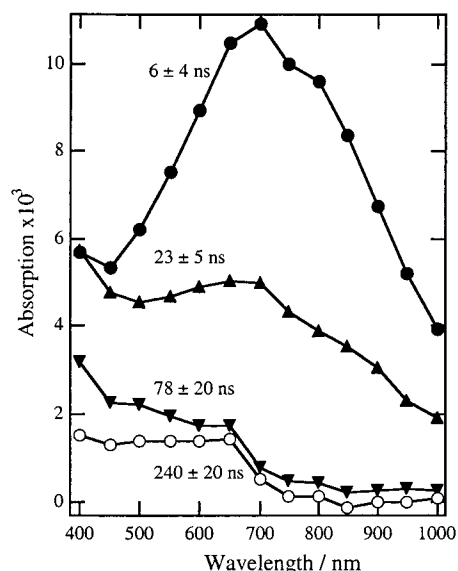
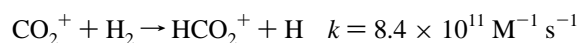


**Figure 3.** Transient spectra observed at four different times in H<sub>2</sub>/CO<sub>2</sub> mixture.

absorption in the wavelength region of interest. There are many organic molecules that can be used as cation scavengers, but these molecules and their cations have strong absorptions in the near UV region. The hydrogen molecule does not suffer from this problem.

In the gas phase, the reaction of CO<sub>2</sub><sup>+</sup> with H<sub>2</sub> has been well studied. CO<sub>2</sub><sup>+</sup> reacts at close to collision-limited rates as<sup>9,49,50</sup>



For (CO<sub>2</sub>)<sub>2</sub><sup>+</sup>, we can expect a similar hydrogen-atom abstraction reaction.<sup>9,51</sup> We can hope that the reaction between H<sub>2</sub> and the anion will be much slower. It is known that the reaction of CO<sub>3</sub><sup>-</sup> with H<sub>2</sub> is quite slow in the gas phase ( $k < 5 \times 10^6 \text{ M}^{-1} \text{ s}^{-1}$ <sup>52</sup>); however, there is no report for the reaction of H<sub>2</sub> with CO<sub>2</sub> anion cluster. Hence, this technique may allow us to extract the anion spectrum.

Figure 3 shows transient spectra measured in a H<sub>2</sub>/CO<sub>2</sub> solution with 160 mM of H<sub>2</sub>. The spectrum immediately after the electron pulse is the same as that measured in pure CO<sub>2</sub>. The spectrum after the (CO<sub>2</sub>)<sub>2</sub><sup>+</sup> decay ( $t > 50$  ns) shows a broad absorption from 650 nm to the UV region and suggests at least one species that is not the cation dimer. As we will discuss below, this spectrum is consistent with photobleaching of infrared spectra of (CO<sub>2</sub>)<sub>2</sub><sup>-</sup>.

**Spectra.** We have been unable to find direct data on the near UV spectrum of (CO<sub>2</sub>)<sub>2</sub><sup>-</sup>. However, there is indirect evidence that comes from the photobleaching of the infrared spectra of (CO<sub>2</sub>)<sub>2</sub><sup>-</sup> in various matrixes. In one study,<sup>43</sup> mercury-arc photolysis with a 470-nm cutoff filter (essentially 546 and 578 nm mercury emission) decreased the (CO<sub>2</sub>)<sub>2</sub><sup>-</sup> infrared bands in an argon matrix about 50%. Irradiation through a 380-nm cutoff filter decreased the infrared bands about 90%, while photolysis with the full arc (240–580 nm) totally removed the (CO<sub>2</sub>)<sub>2</sub><sup>-</sup> infrared bands.

Another confirmation arises from the results of Thompson and Jacox.<sup>45</sup> They measured vibrational spectra of CO<sub>2</sub><sup>+</sup>, C<sub>2</sub>O<sub>4</sub><sup>+</sup>, CO<sub>2</sub><sup>-</sup>, and (CO<sub>2</sub>)<sub>2</sub><sup>-</sup> (which were formed by Penning ionization of a Ne/CO<sub>2</sub> mixture) and observed three different types of photobleaching. The infrared absorption bands for CO<sub>2</sub><sup>-</sup> were diminished by photodetachment after tungsten-lamp irradiation through a 695-nm cutoff. This is interesting because in water



the absorption spectrum of  $\text{CO}_2^-$  is located in the UV region. The IR absorption of the molecular complex (arising from the weak interaction of  $\text{CO}_2^-$  with  $\text{CO}_2$ ) increases on irradiation with light that passes through a 780-nm cutoff filter and decreases with shorter wavelength irradiation. They explained this photobleaching by assuming that the photodetachment of  $\text{CO}_2^-$  occurs by irradiation through a 780 nm cutoff filter and the resulting electrons may be captured by pairs of adjacent  $\text{CO}_2$  molecules to form a  $\text{CO}_2$  anion–molecule complex, which in turn photodetaches at a higher photon energy. Another prominent feature in the infrared, which was assigned to the  $(\text{CO}_2)_2^-$  species, increased after successive tungsten-lamp irradiation through 780-, 695-, and 630-nm cutoff filters and was destroyed by irradiation with a mercury-arc lamp through 420-nm cutoff filter.

Because we expect no significant medium effect from an argon or neon matrix on the absorption spectrum, both experiments suggest that the absorption spectrum of the  $\text{CO}_2^-$  anion cluster is in the visible. We expect the spectra in sc- $\text{CO}_2$  to be similar.

**Possible Role of  $\text{CO}_3^-$ .** One possible intermediate that could appear in the spectrum is  $\text{CO}_3^-$ , a species that is important in the gas phase. This species is formed in the gas phase through the reaction  $\text{O}^- + \text{CO}_2$ . It is known that  $\text{O}^-$  reacts with  $\text{H}_2$  with a reaction rate of  $4.4 \times 10^{10} \text{ M}^{-1} \text{ s}^{-1}$  in the gas phase.<sup>53</sup> Because  $\text{O}^-$  is a precursor for  $\text{CO}_3^-$ , if the spectrum observed in the near UV region were  $\text{CO}_3^-$ , the initial absorption intensity would be decreased by adding  $\text{H}_2$  into  $\text{CO}_2$ . The reported reaction rate of  $\text{O}^-$  with  $\text{CO}_2$  in the gas phase is  $1.6 \times 10^{11} \text{ M}^{-1} \text{ s}^{-1}$ .<sup>54</sup> Using these reaction rates and the concentration of  $\text{H}_2$  and  $\text{CO}_2$ , a reaction probability of  $\text{O}^-$  with  $\text{H}_2$  in  $\text{CO}_2$  under the highest  $\text{H}_2$  concentration is calculated to be about 0.002. (This assumes that the ratio of the reaction rates of  $\text{O}^-$  with the two species is similar in sc- $\text{CO}_2$  and the gas phase.) Therefore, we did not expect  $\text{H}_2$  to scavenge  $\text{O}^-$  under the present experimental conditions.

**3.3. Reactions in  $\text{O}_2/\text{CO}_2$  Mixture.** We have already reported the reaction rate of  $(\text{CO}_2)_2^+$  with  $\text{O}_2$  and found that the reaction rate is  $5 \times 10^{10} \text{ M}^{-1} \text{ s}^{-1}$  in 104 bar of supercritical  $\text{CO}_2$ .<sup>44</sup> In the gas phase, a rate of  $9 \times 10^{10} \text{ M}^{-1} \text{ s}^{-1}$  was reported for the reaction. Because of this relatively fast reaction rate of  $(\text{CO}_2)_2^+$  with  $\text{O}_2$ , we might hope that the spectrum near the UV region could be extracted by eliminating the absorption overlap by the dimer cation. One difference from the  $\text{H}_2/\text{CO}_2$  mixture is that  $\text{O}_2$  will act also as an anion scavenger, which means that the decay kinetics in the near UV might become faster. A second difference is the possible formation of  $\text{CO}_4^-$ .

In Figure 4, the transient spectra and the decay kinetics at 700 and 400 nm are shown. The concentration of  $\text{O}_2$  is approximately 5 mM, and under this condition, the decay at 700 nm is much faster than that at 400 nm. This situation provides us another way to extract the near-UV spectrum without interference from the  $(\text{CO}_2)_2^+$  absorption. The observed spectra are quite similar to the spectra measured in  $\text{H}_2/\text{CO}_2$  mixture, suggesting that the same species are present.

In the presence of  $\text{O}_2$ , one might form  $\text{CO}_4^-$  through the reaction of  $\text{CO}_2^-$  with  $\text{O}_2$ . The photodestruction of  $\text{CO}_4^-$  in solid neon has been previously reported. Vestal and Mauclair<sup>55</sup> found small anion yield in the photodestruction of  $\text{CO}_4^-$  between 600 and 305 nm. However, Moseley and co-workers<sup>56,57</sup> failed to reproduce the ion signal reported by Vestal and Mauclair and concluded that the photodestruction cross section of  $\text{CO}_4^-$  is small over the entire 840 to 350 nm range. Jacox and Thompson<sup>58</sup> found that infrared absorption bands of  $\text{CO}_4^-$  in

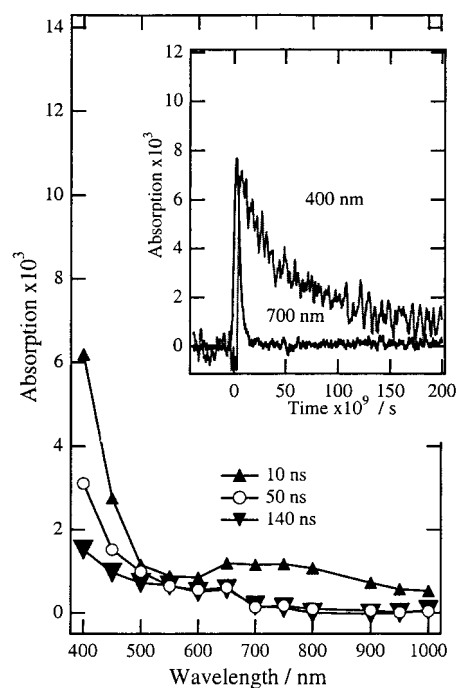


**Figure 4.** Transient spectra observed in  $\text{O}_2/\text{CO}_2$  mixture. The inset shows decay kinetics at 400 and 700 nm.

solid neon could be photobleached by irradiation with a 260-nm cutoff filter, suggesting that absorption of  $\text{CO}_4^-$  is located at a shorter wavelength region than the absorption band of  $(\text{CO}_2)_2^-$ .

Some further evidence that the observed spectrum is not  $\text{CO}_3^-$  has been obtained by examining the reaction rate with  $\text{O}_2$ . From the decay kinetics at 400 nm as a function of the  $\text{O}_2$  concentration, the second-order reaction rate has been estimated as  $2 \times 10^9 \text{ M}^{-1} \text{ s}^{-1}$ . This is similar to but slower than the rate measured by Shkrob and Sauer of  $8 \times 10^9 \text{ M}^{-1} \text{ s}^{-1}$ .<sup>24</sup> By comparing a reported reaction rate for  $\text{CO}_3^-$  with  $\text{O}_2$  in the gas phase<sup>59</sup> ( $k < 3.6 \times 10^6 \text{ M}^{-1} \text{ s}^{-1}$ ), we conclude that the observed rate constant is not that for the reaction of  $\text{O}_2$  with  $\text{CO}_3^-$ . Thus, the absorption spectrum that we measured in the near UV region is expected to arise from  $(\text{CO}_2)_2^-$  (or multimer) and not  $\text{CO}_4^-$  or  $\text{CO}_3^-$ .

So far, we have used  $(\text{CO}_2)_2^-$  to describe the dimer anion. Ab initio calculations predict three different structures for the dimer anion, namely, the symmetrical  $D_{2d}$  and  $D_{2h}$  structures and the asymmetrical  $C_s$  structure.<sup>43,60</sup> For the  $D_{2d}$  and  $D_{2h}$  structures, the excess charge is equally distributed on the two  $\text{CO}_2$  molecules, while in the  $C_s$  asymmetric structure the excess charge is localized in a bending  $\text{CO}_2$  molecule. One would expect that these isomers, which have different charge distributions, would show different electronic absorption spectra. Further, a study by Zhou and Andrew<sup>43</sup> concluded that the  $1665.5 \text{ cm}^{-1}$  band observed on annealing in solid neon is a van der Waals complex of linear  $\text{CO}_2$  and bent  $\text{CO}_2^-$  and  $(\text{CO}_2)_2(\text{CO}_2^-)$  and not the  $C_s$  anion structure characterized by calculation. However, in the photobleaching of those anion clusters in matrixes, there is no clear difference between those dimer anions and a complex because the photobleaching has been done using wide-band cutoff filters. Hence, it is possible that the visible absorption spectra that we measured could include contributions from  $\text{CO}_2$ -anion clusters with different structures. This could be a reason that the spectra measured are broad and asymmetric.

In experiments in which photoionization was used to generate charged species in sc- $\text{CO}_2$  and conductivity was used to observe

the chemistry, Shkrob and Sauer observed a high conductivity species that they assigned to a  $\text{CO}_2^-$  anion.<sup>24</sup> They found that they could photobleach this high conductivity species to generate an even more mobile conduction band electron. The action spectrum for this photoprocess is very similar to that observed for the blue–near-UV species that we have assigned to the dimer anion.

**3.4. Calculation.** There have been many ab initio calculations reported for  $\text{CO}_2^-$ .<sup>26–29</sup> Recently, extensive calculations have been carried out by Gutsev et al.<sup>29</sup> using the infinite-order coupled-cluster method (CCSD) and density functional theory (DFT). The calculated electron affinity of monomeric  $\text{CO}_2$  depends on the model and basis set adopted and ranges between  $-0.48$  and  $-0.69$  eV. (DFT calculation with the B3LYP functional and 6-311+G(2d) basis sets predicts the highest electron affinity ( $-0.48$ ), and the lowest value ( $-0.69$ ) was obtained by CCSD and 6-311+G(3df) basis sets.) These can be compared to the adiabatic electron affinity of monomeric  $\text{CO}_2$ , which has been experimentally determined as  $-0.6 \pm 0.2$ .<sup>25</sup> These calculations have been done for the gas phase. Because we already know that we cannot neglect solvation when we consider the stability of  $\text{CO}_2^-$  anion, we performed calculations including the effects of solvation. In this section, we wish to investigate the energetics of the monomer and dimer anion and the  $\text{CO}_3^-$  and see whether these energetics are consistent with the mechanisms suggested above.

Geometry optimizations for the  $\text{CO}_2$  monomer and dimer anion were performed using the Gaussian 94 program.<sup>61</sup> The B3LYP functional and 6-311+G\* basis sets for C and O atoms were used. After the geometry optimization of the ground state, the potential energy surfaces of  $\text{CO}_2^-$  were calculated. For the dimer anion, three different anion structures are known, namely, the symmetrical  $D_{2d}$  and  $D_{2h}$  anion and the  $C_s$  asymmetrical molecule–anion complex.<sup>41–43</sup>

We adopted the self-consistent isodensity polarized continuum model (SCI-PCM) to consider solvation effects.<sup>62</sup> In this method, the solvent is modeled as a continuum of uniform dielectric constant. The effects of solvation are folded into the iterative SCF computations for the full coupling between the cavity and the electron density. It is well-known that in supercritical fluids there can be considerable clustering of the solvent molecules near a solvent,<sup>63,64</sup> so the uniform dielectric constant may be a poor approximation. The value one should choose for the dielectric constant is not obvious. The bulk value of 1.5 for the dielectric constant is certainly an underestimate. For this reason, we report calculations using 2.0. We have also done the calculations for 1.5, and the conclusions are qualitatively the same.

Figure 5 shows the potential energy surface of  $\text{CO}_2$  and  $\text{CO}_2^-$  anion as a function of  $\text{O}=\text{C}=\text{O}$  angle. The zero of energy was selected so that the ground-state  $\text{CO}_2$  is 0 eV. Also included are results for solvent effects using the SCI-PCM model. The bond lengths were optimized at each angle.

In the gas phase, the energy of  $\text{CO}_2^-$  in its ground state (bent) is 0.37 eV above the ground state of linear neutral  $\text{CO}_2$ . The lowest point of crossing between the energy surfaces of  $\text{CO}_2^-$  and  $\text{CO}_2$  occurs at a bond angle of about  $152^\circ$ .  $\text{CO}_2^-$  can be formed if its vibrational excitation energy exceeds approximately 0.58 eV. However, the activation energy for autodetachment is 0.21 eV. This low activation energy for the autodetachment is the reason that the lifetime of  $\text{CO}_2^-$  is quite short and  $\text{CO}_2^-$  is unstable in the gas phase.

On the other hand, in a dielectric continuum solvent, the energy of  $\text{CO}_2^-$  in its ground state is 0.76 eV below the ground

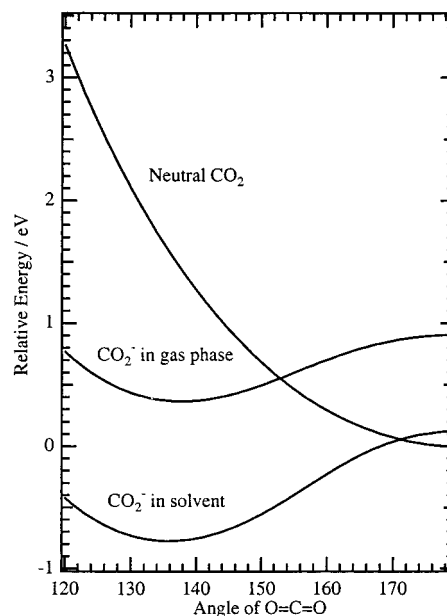


**Figure 5.** Potential energy surfaces of  $\text{CO}_2$ ,  $\text{CO}_2^-$  in the gas phase and  $\text{CO}_2^-$  in a solvent as a function of the  $\text{OCO}$  angle. The energies are scaled so that the ground state of  $\text{CO}_2$  is 0 eV.

state of neutral  $\text{CO}_2$ . Because a system that has a zero dipole moment will not exhibit a solvent effect for the SCI-PCM model, the calculations for neutral  $\text{CO}_2$  are the same in the solvent and the gas phase. The lowest point of crossing between the surfaces occurs at bond angle of  $171^\circ$ , significantly closer to the linear  $\text{O}=\text{C}=\text{O}$  angle than that calculated for the gas phase. Another important difference from the gas-phase result is that the activation energy for autodetachment is 0.89 eV. This means that the solvated  $\text{CO}_2^-$  is stable to autodetachment rather than metastable. These calculation results are consistent with experimental observation of  $\text{CO}_2^-$  in nonpolar organic liquid<sup>65</sup> and supercritical ethane<sup>66</sup> and explain why  $\text{CO}_2^-$  is stable in such media. There is no reason that we cannot expect similar stabilization of  $\text{CO}_2^-$  in supercritical  $\text{CO}_2$ .

The adiabatic electron affinity,  $\text{EA}_{\text{ad}}$ , for the dimer can be calculated within the Born–Oppenheimer approximation as

$$\text{EA}_{\text{ad}} = E_{\text{total}}(\text{neutral}) + \text{ZPE}(\text{neutral}) - E_{\text{total}}(\text{anion}) - \text{ZPE}(\text{anion})$$

where  $\text{ZPE}$  is zero point vibrational energy and can be estimated within the harmonic approximation. The energy of the neutral  $\text{CO}_2$  dimer at the B3LYP/6-311+G\* level is calculated to be  $-377.271\,006$  hartree, and the zero point energy is  $0.023\,602$  hartree, where the neutral dimer structure is the *slipped parallel* geometry.<sup>67,68</sup> It is known that the  $D_{2d}$   $\text{C}_2\text{O}_4^-$  is more stable than the  $C_s$  and  $D_{2h}$  forms, so we only calculated for the  $D_{2d}$  symmetry. From its total energy ( $-377.303\,144\,928$ ) and zero point energy ( $0.023\,127$ ), the electron affinity of  $D_{2d}$   $\text{C}_2\text{O}_4^-$  is calculated to be 0.89 eV. The experimentally determined value of 0.8 eV has been reported by Quitevis and Herschbach,<sup>40</sup> who measured the charge-transfer reaction from alkali atoms to the weakly bound  $\text{CO}_2$  cluster. Surprisingly, the calculated and measured values are identical. Therefore, one can expect that even in the gas phase,  $\text{CO}_2$  dimer can capture an electron and form a stable dimer anion. We expect that the dimer anion will be more stable in the supercritical fluid, much like the monomer anion calculated above.

We can put some experimental limits on the electron affinity for the dimer in a sc- $\text{CO}_2$  solution. We previously studied the

reduction of *p*-benzoquinone (*p*-BQ) in supercritical CO<sub>2</sub> and observed the spectrum of the *p*-BQ anion.<sup>44</sup> The formation of *p*-BQ anion was tentatively assigned as the result of an electron-transfer reaction from CO<sub>2</sub> dimer anion to *p*-BQ. However, we were unable to observe anions for pyrene and naphthalene molecules, whose electron affinities are smaller than that of *p*-BQ. The adiabatic electron affinity of *p*-BQ is reported as 1.8–1.9 eV,<sup>69</sup> whereas the electron affinities of pyrene and naphthalene are 0.50–0.59<sup>69</sup> and 0.13–0.15 eV,<sup>69</sup> respectively. If we assume that the solvation energy is not significantly different for those molecular systems, the failure to form an anion may be due to the fact that the electron affinity of the anion is higher than that of naphthalene and pyrene. Thus, the electron affinity of the dimer anion can be expected to be located between 0.5 and 1.9 eV. This range certainly is consistent with the electron affinity suggested by the theoretical calculations.

We can also investigate the properties and possible reactions of CO<sub>3</sub><sup>-</sup>. The electron affinity of CO<sub>3</sub> may also be computed as the energy difference between the neutral form and the anion. The energies of CO<sub>3</sub> and its zero point energy are calculated to be -263.714 84 and 0.012 68 hartree, respectively, at the B3LYP/6-311+G\* level. For CO<sub>3</sub><sup>-</sup>, the corresponding energies are -263.902 15 and 0.011 95 hartree, respectively. Therefore, the electron affinity of CO<sub>3</sub> is calculated to be 5.12 eV. The experimentally determined electron affinity value ranges between 2.7 and 3.3 eV.<sup>69</sup> This large electron affinity suggests that CO<sub>3</sub><sup>-</sup> is very stable, and it is energetically unlikely to transfer the electron to molecules such as *p*-BQ the electron affinity of which is considerably smaller.

#### 4. Conclusion

We have studied transient absorption spectra produced within a few hundred nanoseconds of the radiolysis of supercritical CO<sub>2</sub> and CO<sub>2</sub> mixtures. As previously discussed, the main cationic species is (CO<sub>2</sub>)<sub>2</sub><sup>+</sup> with an absorption maximum at 700 nm. For negative ions, we assigned the primary transient species to the (CO<sub>2</sub>)<sub>2</sub><sup>-</sup> or CO<sub>2</sub> anion–molecule complex. The absorption starts around 650 nm, and the spectral shape is broad, as shown in Figure 3. The anion clusters react with O<sub>2</sub> with a rate constant of approximately  $2 \times 10^9 \text{ M}^{-1} \text{ s}^{-1}$  at 104 bar and 40.1 °C. The density functional calculation including solvation predicts that CO<sub>2</sub><sup>-</sup> is stable to autodetachment in a continuum solvent of which the dielectric constant is 2.0. The calculations also predict a positive electron affinity (0.89 eV) for the CO<sub>2</sub> dimer.

In this article, we have not discussed the formation mechanisms of the anion cluster in supercritical CO<sub>2</sub>. In the cluster experiments, one mechanism is the attachment of a thermalized electron to a neutral CO<sub>2</sub> cluster. Another possible mechanism is the attachment of a relatively high-energy electron to a neutral CO<sub>2</sub> cluster, as has been observed by Klots and Compton. We think that both formation mechanisms can occur in the radiolysis of supercritical CO<sub>2</sub> because secondary electrons are distributed over a wide energy range and CO<sub>2</sub> clusters are formed in supercritical CO<sub>2</sub>. We plan to examine the formation mechanism using several electron scavengers the electron-capture cross sections of which are different.

Finally, the question of the formation of CO<sub>3</sub><sup>-</sup> in sc-CO<sub>2</sub> radiolysis remains. While it is an important species in the radiolysis of gas-phase CO<sub>2</sub>, there is no evidence for its formation in the radiolysis of sc-CO<sub>2</sub>.

**Acknowledgment.** We acknowledge Dr. Sergey Chemerisov for operation of the accelerator. Acknowledgment is also made to Argonne National Laboratory, The Department of Energy,

and the Ministry of Education in Japan for financial support to K.T. All of the calculations were done using the computer center in Hokkaido University.

#### References and Notes

- (1) Kajimoto, O. *Chem. Rev.* **1999**, *99*, 355.
- (2) Tucker, S. C. *Chem. Rev.* **1999**, *99*, 391.
- (3) Brennecke, J. F.; Chateaufneuf, J. E. *Chem. Rev.* **1999**, *99*, 433.
- (4) Kimura, Y.; Takebayashi, Y.; Hirota, N. *J. Chem. Phys.* **1998**, *108*, 1485.
- (5) Sasaki, A.; Kudoh, H.; Senboku, H.; Tokuda, M. Electrochemical carboxylation of several organic halides in supercritical carbon dioxide. In *Novel Trends in Electroorganic Synthesis*; Torii, S., Ed.; Springer: Tokyo, 1998; p 245.
- (6) Mori, Y.; Szalda, D. J.; Brunschwig, B. S.; Schwarz, H. A.; Fujita, E. Towards the photoreduction of CO<sub>2</sub> with Ni(2,2'-bipyridine)<sub>n</sub><sup>2+</sup> complexes. In *Photochemistry and Radiation Chemistry: Complementary Methods for the Study of Electron Transfer*; Wishart, J. F., Nocera, D. G., Eds.; American Chemical Society: Washington, DC, 1998; Vol. 254, p 279.
- (7) Fujita, E. *Coord. Chem. Rev.* **1999**, *185/186*, 373.
- (8) Wickham, A. J.; Best, J. V.; Wood, C. J. *Radiat. Phys. Chem.* **1977**, *10*, 107.
- (9) Norfolk, D. J.; Skinner, R. F.; Williams, W. J. *Radiat. Phys. Chem.* **1983**, *21*, 307.
- (10) Rakshit, A. B.; Warneck, P. Z. *Naturforsch.* **1979**, *34A*, 1410.
- (11) Willis, C.; Bindner, P. E. *Can. J. Chem.* **1970**, *48*, 3463.
- (12) Willis, C.; Boyd, A. W.; Bindner, P. E. *Can. J. Chem.* **1970**, *48*, 1951.
- (13) Kummeler, R.; Leffert, C.; Im, K.; Piccirelli, R.; Kevan, L.; Willis, C. J. *Phys. Chem.* **1977**, *81*, 2451.
- (14) Ikezoe, Y.; Shimizu, S.; Sato, S.; Matsuoka, S.; Nakamura, H.; Tamura, T. *Radiat. Phys. Chem.* **1982**, *20*, 253.
- (15) Ikezoe, Y.; Onuki, K.; Shimizu, S.; Nakajima, H.; Sato, S.; Matsuoka, S.; Nakamura, H.; Tamura, T. *Radiat. Phys. Chem.* **1985**, *26*, 445.
- (16) Parkes, D. A. *J. Chem. Soc., Faraday Trans. 1* **1972**, *68*, 627.
- (17) Parkes, D. A. *J. Chem. Soc., Faraday Trans. 1* **1973**, *69*, 198.
- (18) Knapp, M.; Echt, O.; Kreisle, D.; Mark, T. D.; Recknagel, E. *Chem. Phys. Lett.* **1986**, *126*, 225.
- (19) Baulch, D. L.; Dainton, F. S.; Willix, R. L. S. *Trans. Faraday Soc.* **1965**, *61*, 1146.
- (20) Yoshimura, M.; Chosa, M.; Soma, Y.; Nishikawa, M. *J. Chem. Phys.* **1972**, *57*, 1626.
- (21) Jacobsen, F. M.; Freeman, G. R. *J. Chem. Phys.* **1986**, *84*, 3396.
- (22) Kumar, S. V. K.; Venkatasubramanian, V. S. *J. Chem. Phys.* **1983**, *79*, 6423.
- (23) Schroder, D.; Shalley, C. A.; Harvey, J. N.; Schwarz, H. *Int. J. Mass Spectrom.* **1999**, *185/186/187*, 25.
- (24) Shkrob, I. A.; Sauer, M. C., Jr. *J. Phys. Chem. B* **2001**, *105*, 4520.
- (25) Compton, R. N.; Reinhardt, P. W.; Cooper, C. D. *J. Chem. Phys.* **1975**, *63*, 3821.
- (26) England, W. B.; Rosenberg, B. J.; Fortune, P. J.; Wahl, A. C. *J. Chem. Phys.* **1976**, *65*, 684.
- (27) Pacansky, J.; Wahlgren, U.; Bagus, P. S. *J. Chem. Phys.* **1975**, *62*, 2740.
- (28) Yu, D.; Rauk, A.; Armstrong, D. A. *J. Phys. Chem.* **1992**, *96*, 6031.
- (29) Gutsev, G. L.; Bartlett, R.; Compton, R. N. *J. Chem. Phys.* **1998**, *108*, 6756.
- (30) Klots, C. E.; Compton, R. N. *J. Chem. Phys.* **1977**, *67*, 1779.
- (31) Klots, C. E.; Compton, R. N. *J. Chem. Phys.* **1978**, *69*, 1636.
- (32) Klots, C. E. *Radiat. Phys. Chem.* **1982**, *20*, 51.
- (33) Stamatovic, A.; Stephan, K.; Mark, T. D. *Int. J. Mass Spectrom.* **1985**, *63*, 37.
- (34) Stamatovic, A.; Leiter, K.; Ritter, W.; Stephan, K.; Mark, T. D. *J. Chem. Phys.* **1985**, *83*, 2942.
- (35) Misaizu, F.; Mitsuke, K.; Kondow, T.; Kuchitsu, K. *J. Chem. Phys.* **1991**, *94*, 243.
- (36) Tsukuda, T.; Johnson, M. A.; Nagata, T. *Chem. Phys. Lett.* **1997**, *268*, 429.
- (37) Hatano, Y.; Shimamori, H. Electron attachment in dense gases. In *Electron and ion swarms*; Christophorou, L. G., Ed.; Pergamon: New York, 1981.
- (38) Tsukuda, M.; Shima, N.; Tsuneyuki, S.; Kageshima, H. *J. Chem. Phys.* **1987**, *87*, 3927.
- (39) Bowen, K. H.; Liesegang, G. W.; Sanders, R. A.; Herschbach, D. R. *J. Phys. Chem.* **1983**, *87*, 557.
- (40) Quitevis, E. L.; Herschbach, D. R. *J. Phys. Chem.* **1989**, *93*, 1136.
- (41) Rossi, A. R.; Jordan, K. D. *J. Chem. Phys.* **1979**, *70*, 4422.
- (42) Saeki, M.; Tsukuda, T.; Iwata, S.; Nagata, T. *J. Chem. Phys.* **1999**, *111*, 6333.



- (43) Zhou, M.; Andrews, L. *J. Chem. Phys.* **1999**, *110*, 2414.
- (44) Dimitrijevic, N. D.; Takahashi, K.; Bartels, D. M.; Jonah, C. D.; Trifunac, A. D. *J. Phys. Chem. A* **2000**, *104*, 568.
- (45) Thompson, W. E.; Jacox, M. E. *J. Chem. Phys.* **1999**, *111*, 4487.
- (46) Zhou, M.; Andrews, L. *J. Chem. Phys.* **1999**, *110*, 6820.
- (47) Dimitrijevic, N. M.; Bartels, D. M.; Jonah, C. D.; Takahashi, K. *Chem. Phys. Lett.* **1999**, *309*, 61.
- (48) Smith, G. P.; Lee, L. C. *J. Chem. Phys.* **1978**, *69*, 5393.
- (49) Fehsenfeld, F. C.; Schmeltekopf, A. L.; Ferguson, E. E. *J. Chem. Phys.* **1967**, *46*, 2802.
- (50) Rakshit, A. B.; Warneck, P. *J. Chem. Soc., Faraday Trans. 2* **1980**, *76*, 1084.
- (51) Meo-Ner, M.; Field, F. H. *J. Chem. Phys.* **1977**, *66*, 4527.
- (52) Price, D. A.; Moruzzi, J. L. *Vacuum* **1974**, *24*, 591.
- (53) Parkes, D. A. *J. Chem. Soc., Faraday Trans. 1* **1972**, *68*, 613.
- (54) Moruzzi, J. L.; Phelps, A. V. *Bull. Am. Phys. Soc.* **1966**, *11*, 506.
- (55) Vestal, M. L.; Mauclaire, G. H. *J. Chem. Phys.* **1977**, *67*, 3758.
- (56) Smith, G. P.; Lee, L. C.; Cosby, P. C.; Peterson, J. R.; Moseley, J. T. *J. Chem. Phys.* **1978**, *68*, 3818.
- (57) Smith, G. P.; Lee, L. C.; Mosely, J. T. *J. Chem. Phys.* **1979**, *65*, 5267.
- (58) Jacox, M. E.; Thompson, W. E. *J. Phys. Chem.* **1991**, *95*, 2781.
- (59) Dotan, I.; Davidson, J. A.; Streit, G. E.; Albritton, D. L.; Fehsenfeld, F. C. *J. Chem. Phys.* **1977**, *67*, 2874.
- (60) Fleischman, S. H.; Jordan, K. D. *J. Phys. Chem.* **1987**, *91*, 1300.
- (61) Frisch, M. J.; Trucks, G. W.; Schlegel, H. B.; Gill, P. M. W.; Johnson, B. G.; Robb, M. A.; Cheeseman, J. R.; Keith, T.; Petersson, G. A.; Montgomery, J. A.; Raghavachari, K.; Al-Laham, M. A.; Zakrzewski, V. G.; Ortiz, J. V.; Foresman, J. B.; Cioslowski, J.; Stefanov, B. B.; Nanayakkara, A.; Challacombe, M.; Peng, C. Y.; Ayala, P. Y.; Chen, W.; Wong, M. W.; Andres, J. L.; Replogle, E. S.; Gomperts, R.; Martin, R. L.; Fox, D. J.; Binkley, J. S.; Defrees, D. J.; Baker, J.; Stewart, J. P.; Head-Gordon, M.; Gonzalez, C.; Pople, J. A. *Gaussian 94*, revision E.2; Gaussian, Inc.: Pittsburgh, PA, 1995.
- (62) Foresman, J. B.; Keith, T. A.; Wiberg, K. B. *J. Phys. Chem.* **1996**, *100*, 16098.
- (63) Itoh, K.; Holroyd, R. A.; Nishikawa, M. *J. Phys. Chem. A* **2001**, *105*, 703.
- (64) Takahashi, K.; Abe, K.; Sawamura, S.; Jonah, C. D. *Chem. Phys. Lett.* **1998**, *282*, 361.
- (65) Nishikawa, M.; Itoh, K.; Holroyd, R. A. *J. Phys. Chem.* **1988**, *92*, 5262.
- (66) Nishikawa, M.; Itoh, K.; Holroyd, R. A. *J. Phys. Chem. A* **1999**, *103*, 550.
- (67) Jucks, K. W.; Huang, Z. S.; Dayton, D.; Miller, R. E.; Lafferty, W. J. *J. Phys. Chem.* **1987**, *86*, 4341.
- (68) Illies, A. J.; McKee, M. L.; Schlegel, H. B. *J. Phys. Chem.* **1987**, *91*, 3489.
- (69) Lias, S. G.; Bartmess, J. E.; Liebman, J. F.; Holmes, J. J.; Levin, R. D.; Mallard, W. G. *J. Phys. Chem. Ref. Data* **1988**, *17* (Suppl. 1).